Table 2. Prohapten and photohapten in photopatch test

	Photopatch test	Patch test of UV-preirradiated chemical
Prohapten	− (or +)	+
Photohapten	+	−

plied to the skin as patch test. Empirically, photopatch test has been performed to test the photoallergenicity of chemicals. Our studies have suggested that the vast majority of clinically photoallergic chemicals are photohaptens rather than prohaptens (11-13). Therefore, patients mostly exhibit positive photopatch test but negative patch test of the preirradiated chemical (Table 2).

Mouse model of photoallergic contact dermatitis

Mouse models of photoallergic contact dermatitis were established by several groups in the early 1980's (14, 15), and enabled researchers to elucidate mechanisms of the sensitivity, because of its technical convenience and availability of accumulated immunologic information on this species. In these models, 3,3',4',5-tetrachlorosalicylanilide (TCSA), a representative halogenated salicylanilide, has been used typically as photohapten. Mice are sensitized by 2 daily abdominal paintings with 1% of TCSA plus UVA irradiation and challenged 5-days later on the earlobes with TCSA plus UVA. Ear swelling responses are measured 24 h after challenge. In addition to TCSA, the photoallergenic potential of other halogenated salicylanilides, such as tribromosalicylanilide and bithionol, is also detected by this mode of sensitization (16).

Murine photoallergic contact dermatitis to TCSA is genetically controlled and determined mainly by the major histocompatibility complex (MHC) (17, 18). Mice with H-$2^{b,d}$ alleles are high responders, whereas the H-2^{k} haplotype is closely associated with low responders (18). Such a clear-cut association of the H-2 haplotype with the degree of response has not been found in ordinary contact dermatitis to haptens. We have recently found that in photoallergic contact dermatitis to ketoprofen, a non-steroidal anti-inflammatory drug, mice with H-2^{k} are high responders, whereas those with H-$2^{b,d}$ are low responders. Therefore, high responder H-2 haplotypes differ among photosensitivities to each photohaptenic chemical.

Immunological mechanism of photoallergic contact dermatitis

UVA is the action spectrum of this photoderivatization, as protein and cells are photocoupled with a photohapten by irradiation with UVA but not UVB. The main sequential events in photoallergic contact dermatitis are virtually the same as those of ordinary contact dermatitis except for the requirement of UV irradiation in sensitization and challenge (Fig. 2). Photoconjugation of epidermal cells with TCSA is the initial step in the photoallergy. Langerhans cells (LC), which are professional antigen-presenting cells in the epidermis, play an important role and T cells sensitized by photohapten-bearing LC induce this photosensitivity (2). Migration of TCSA-bearing LC to draining lymph nodes in the sensitization phase (19) and involvement of mast cells in the challenge phase (20) are requirements.

Murine photoallergic contact dermatitis to TCSA involves both positive and negative immunologic pathways that are restricted by I-A and I-E molecules on antigen-presenting cells (18, 21). The suppressive pathway is mediated by IL-10-producing Th2 cells (21), which had been known as suppressor T cells and may correspond to recently called regulatory T cells. Sensitization with TCSA plus UVA is prone to induce Th2 cells compared to ordinary haptens

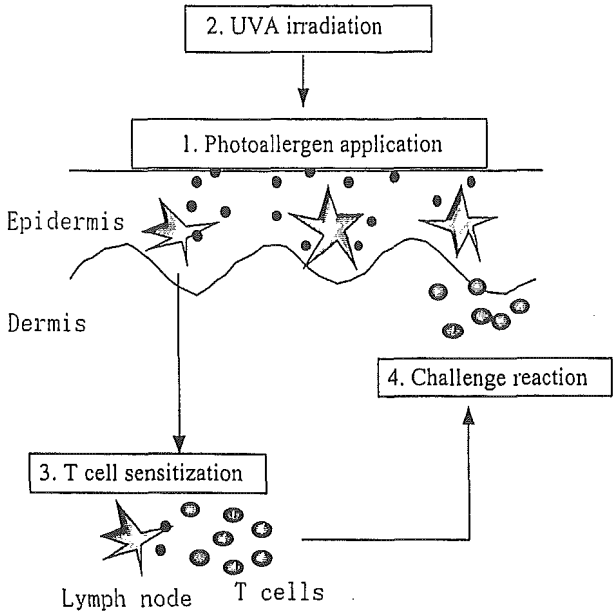

Fig. 2 Immunological mechanism of photoallergic contact dermatitis

(22), suggesting that the suppressive immunologic pathway is clearly detectable in this sensitivity. Antigen-specific, afferent limb-acting Th2 or regulatory T cells are responsible for the low responsiveness of H-2^k mice. The low responsiveness of photoallergic contact dermatitis in the H-2^k strain is due to the preferential activation of Th2 or regulatory T cells via I-E^k molecules (18).

Molecular mechanism of photoantigen presentation

In photoallergic contact dermatitis and drug photoallergy, causative photohaptens are bound to MHC class II molecules/self peptide on LC upon exposure to UVA (23). The photomodified LC sensitize and elicit antigen-specific T cells that mediate photoallergy (24). In our murine model of fluoroquinolone photoallergy, quinolone diffuses to the epidermis. Upon UVA exposure, LC are photomodified with a given quinolone in their MHC class II-associated peptides, thereby sensitizing and eliciting TCR V β 13-bearing T cells (25), which lead to photoallergic skin reactions. It is possible that protein is covalently bound to a photodegradated site of photohapten to form an allergic photohapten-protein complex (25). Lysine is a preferential amino acid to afford the binding site to a photohapten (23). Primed $CD4^+$ T cells proliferated *in vitro* in response to LC loaded with class II (I-A^d)-binding, lysine-containing peptides when photomodified with a photohapten (23). Epicutaneous application of the FQ-photoconjugated peptide *via* barrier-disrupted skin was able to sensitize mice for subsequent elicitation of photoallergy evoked with systemic photohapten and UVA.

Topical application of TCSA and UVA irradiation not only produce the formation of photoantigen but also promote the antigen-presenting ability of LC. The combination of TCSA painting and UVA exposure markedly elevates the expression of MHC class II and CD86 and slightly that of CD80 and CD54 on the surface of LC (26). There exist subpopulations of LC that express MHC class II and CD86 at high levels. Since neither TCSA painting nor UVA exposure alone enhances the expression, both treatments are essential for enhancement. MHC class II and CD86 molecules are mandatory for the antigen-presenting function of LC. Therefore, as ordinary haptens (27), photohaptens are capable of inducing immunocompetent molecules on antigen-

presenting cells when irradiated with UVA.

Future study: Screening of photoallergenicity using *in vitro* system

The phototoxicity of given substances has been evaluated in many *in vitro* systems, and the standard system is now being established by using cellular phototoxicity. However, the photoallergenicity is not easily evaluated in either *in vivo* or *in vitro* system. In particular, it is very difficult for an *in vitro* system to predict photoallergenicity. Nonetheless, two possibilities may be proposed for the prediction. One is to test photoconjugation of given substances with protein, because this binding is the initial step of photoallergy in the skin and yields photoantigens. Liquid chromatography or mass spectrometry is a choice to examine the conjugation. In the other system, some cell lines with antigen-presenting ability, such as THP-1, can be used for *in vitro* treatment with a photoallergic substance plus UVA. When the phototreated cells express higher levels of MHC class II and costimulatory molecules, such as CD86, CD80 or CD40, the substance will have an ability to phosensitize and photoelicit T cells. These systems may shed light for future studies.

References

1. Yamamoto O, Tokura Y: Photocontact dermatitis and chloracne: two major occupational and environmental skin diseases induced by different actions of halogenated chemicals, J Dermatol Sci 32: 85-94, 2003
2. Tokura Y, Takigawa M: Immunological mechanisms of contact photosensitivity, Eur J Dermatol 3: 87-91, 1993
3. Epstein J H: Photoallergy: a review, Arch Dermatol 106: 741-747, 1972
4. Zugerman C: Dermatology in the workplace, Am Fam Physician 26: 103-109, 1982
5. Tokura Y: Immune responses to photohaptens: implications for the mechanisms of photosensitivity to exogenous agents, J Dermatol Sci 23 suppl: 6-9, 2000
6. Wilkinson D S: Photodermatitis due to tetrachlorosalicylanilide, Br J Dermatol 73: 213-219, 1961
7. Harber L C, Harris H, Baer R L: Photoallergic contact dermatitis due to halogenated salicylanilides and related compounds, Arch Dermatol 94: 255-262, 1966
8. Epstein J H, Wepper K D, Maibach H I: Photocontact dermatitis to halogenated salicylanilides and related compounds: a clinical and histological review of 26 patients, Arch Dermatol 97: 236-244, 1968
9. Bosca F, Miranda M A: Photosensitizing drugs containing the benzophenone chromophore, J Photochem Photobiol B 43: 1-26, 1998
10. Fujita H, Matsuo I: Type I lipid photooxidation by the nonsteroidal anti-inflammatory drug suprofen: a possible key to its photosensitivity, Photodermatol Photoimmunol Photomed 9: 203-208, 1993
11. Tokura Y, Takigawa M, Yamada M: Induction of contact photosensitivity to TCSA using photohapten-modified syngeneic spleen cells, Arch Dermatol Res 280: 207-213, 1988
12. Tokura Y, Ogai M, Yagi H, et al: Afloqualone photosensitivity: Immunogenicity of afloqualone-photomodified epidermal cells, Photochem Photobiol 60: 262-267, 1994
13. Tokura Y, Nishijima T, Yagi H, et al: Photohaptenic properties of fluoroquinolones, Photochem Photobiol 64: 838-844, 1996
14. Takigawa M, Miyachi Y: Mechanisms of contact photosensitivity in mice: I. T cell regulation of contact photosensitivity to tetrachlorosalicylanilide under the genetic restrictions of the major histocompatibility complex, J Invest Dermatol 79: 108-115, 1982
15. Maguire H C, Kaidbey K: Experimental photoallergic contact dermatitis: a mouse model, J Invest Dermatol 79: 147-152, 1982
16. Miyachi Y, Takigawa M: Mechanisms of contact photosensitivity in mice. III. Predictive testing of chemicals with photoallergenic potential in mice, Arch Dermatol 119: 736-739, 1983
17. Tokura Y, Satoh T, Yamada M, et al: Genetic control of contact photosensitivity to tetrachlorosalicylanilide. II. Igh complexes controls the sensitivity induced by photohapten-modified spleen cells but not epidermal cells, Cell Immunol 135: 195-207, 1991
18. Tokura Y, Satoh T, Takigawa M, et al: Genetic control of contact photosensitivity to tetrachlorosalicylanilide. I. Preferential activation

of suppressor T cells in low responder H-2^k mice, J Invest Dermatol 94: 471-476, 1990
19. Gerberick G F, Ryan C A, Fletcher E R, et al: Increased number of dendritic cells in draining lymph nodes accompanies the generation of contact photosensitivity, J Invest Dermatol 96: 355-361, 1991
20. Miyachi Y, Imamura S, Tokura Y, et al: Mechanisms of contact photosensitivity in mice. VII. Diminished elicitation by reserpine and defective expression in mast cell-deficient mice, J Invest Dermatol 87: 39-41, 1986
21. Yagi H, Tokura Y, Wakita H, et al: TCRV β 7+ Th2 cells mediate UVB-induced suppression of murine contact photosensitivity by releasing IL-10, J Immunol 156: 1824-1831, 1996
22. Suzuki K, Yamazaki S, Tokura Y: Expression of T-cell cytokines in challenged skin of murine allergic contact photosensitivity: low responsiveness is associated with induction of Th2 cytokines, J Dermatol Sci 23: 138-144, 2000
23. Tokura Y, Seo N, Fujie M, et al: Quinolone-photoconjugated MHC class II- bearing peptides with lysine are antigenic for T cells mediating murine quinolone photoallergy, J Invest Dermatol 117: 1206-1211, 2001
24. Ohshima A, Seo N, Takigawa M, et al: Formation of antigenic quinolone photoadducts on Langerhans cells initiates photoallergy to systemically administered quinolone in mice, J Invest Dermatol 114: 569-575, 2000
25. Tokura Y, Seo N, Yagi H, et al: Cross-reactivity in murine fluoroquinolone photoallergy: exclusive usage of TCR Vß13 by immune T cells that recognize fluoroquinolone-photomodified cells, J Immunol 160: 3719-3728, 1998
26. Nishijima T, Tokura Y, Imokawa G, et al: Photohapten TCSA painting plus UVA irradiation of murine skin augments the expression of MHC class II molecules and CD86 on Langerhans cells, J Dermatol Sci 19: 202-207, 1999
27. Aiba S, Katz S I: Phenotypic and functional characteristics of in vivo-activated Langerhans cells, J Immunol 145: 2791-2796, 1990

Journal of Dermatological Science (2005) 40, 59–61

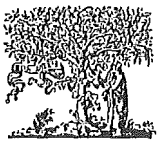

ELSEVIER

Journal of Dermatological SCIENCE

www.intl.elsevierhealth.com/journals/jods

LETTER TO THE EDITOR

Journal of Dermatological Science (2005) 40, 59–61

ELSEVIER

Journal of Dermatological SCIENCE

www.intl.elsevierhealth.com/journals/jods

LETTER TO THE EDITOR

The role of low-density lipoprotein receptors in sensitivity to killing by Photofrin-mediated photodynamic therapy in cultured human tumor cell lines

Photodynamic therapy (PDT) is a newly developed modality for the treatment of patients with cancer [1]. Recently a partially purified fraction of the hematoporphyrin derivatives, Photofrin®, has frequently been used as a photosensitizer in PDT. There are several rationales for which Photofrin-PDT exerts its therapeutic effectiveness: (1) Photofrin accumulates selectively into cancer cells through low-density lipoprotein receptors (LDL-R); (2) reactive oxygen species (ROS) generated after the photoexcitation of Photofrin by laser irradiation destroy tumor cells; (3) vascular tissues necessary for tumor growth can be injured by Photofrin-PDT, resulting in the occlusion of vessels [2–6]. However, the precise mechanisms of Photofrin-PDT-induced tumor-cell killing have not yet been fully elucidated. The important clinical aspect is to clarify whether Photofrin-PDT sensitivity differs among various tumors and to predict which types of tumors are more effectively treated with Photofrin-PDT. Furthermore, the significance of LDL-R at the surface of tumor cells for the incorporation of Photofrin and the resultant effectiveness of Photofrin-PDT still remains controversial [2,7,8]. To better understand Photofrin-PDT in the above respects, we examined the effectiveness of in vitro Photofrin-PDT in cultured human tumor cell lines and analyzed the sensitivity of Photofrin-PDT in relation to their expression of LDL-R and uptake of Photofrin.

Human tumor cell lines and a normal fibroblast cell line used in the study are listed in Table 1. The cells were maintained in Dulbecco's modified minimum essential medium (DMEM) (Sigma Chemical CC, Tokyo, Japan) with 10% fetal bovine serum (Filtron, Australia) at 37 °C in a 5% CO_2 atmosphere.

Immunohistochemically, the expression of LDL-R in squamous cell carcinoma (SCC) cells (HSC-2) and adenocarcinoma cells (MKN45) was high, while melanoma cell lines (G361, Mewo and C32TG) and normal cells (N-1) bore the receptor at very low or even undetectable levels by use of polyclonal antibody to human LDL-R (working dilution; 1:10, Progen, Heiderberg, Germany). Using the fluorescence microscopy [9], the uptake of Photofrin (Wyeth-Lederle, Japan, 50 μg/ml at 37 °C for 1 h in DMEM) into the cells was higher in SCC cells (HSC-2) and relatively higher in adenocarcinoma cells (MKN45) than that in melanoma cells (G361, C32TG). The fluorescence of Photofrin was barely detectable in normal cells (N-1). The intensity of fluorescence in MKN45 was detectable but less intensive than that in HSC-2. When HSC-2 and G361 were treated in the presence of LDL (0.5 mg protein/ml in DMEM, Sigma–Aldrich, St. Louis, MO, USA) with Photofrin, the uptake of Photofrin into SCC cells (HSC-2) was much decreased with the LDL treatment compared to that without LDL treatment. However, HDL (1 mg protein/ml in DMEM, Sigma–Aldrich, St. Louis, MO, USA) did not affect the uptake of Photofrin in SCC cells (HSC-2).

Cells were treated with Photofrin (50 μg/ml at 37 °C for 1 h in DMEM), washed by phosphate-buffered saline and irradiated with an optical parametric oscillator (OPO) laser (Hamamatsu Photonics K.K., Hamamatsu, Japan) emitting 7.3 mW/cm^2 of the energy fluence rate at 630 nm. At this irradiance, the hyperthermic effect of Photofrin-PDTwas negligible. Five days after the treatment, cell survival was determined as described previously [10]. Survival was expressed as the ratio of cell counts in the treated dishes to that in the control (Photofrin treatment without laser irradiation) dishes. Survival affected by laser irradiation without Photofrin treatment was also measured. Our preliminary study showed that 50 μg/ml or less of Photofrin treatment for 1 h without subsequent laser irradiation had no cytotoxic effect on HSC-2. As shown in the figure, in vitro Photofrin-PDT killed cultured tumor cells and the sensitivity to Photofrin-PDT varied widely among the cultured human cell lines. The post-Photofrin-PDT survivals of human SCC (HSC-2 and HSC-3) and

0923-1811/$30.00
doi:10.1016/j.jdermsci.2005.01.009

Table 1 Characteristics of cell lines used in the study

Cell strain	Type of tumor (histopathology and origin)	Sources#	LDL-R*1	Uptake of Photofrin*2		
				No treatment	+LDL	+HDL
HSC-2	Squamous cell carcinoma (lip)	JCRB (0622)	++	++	±	++
HSC-3	Squamous cell carcinoma (tongue)	JCRB (0623)	n.d.	n.d.	n.d.	n.d.
Mewo	Melanoma (lymph node)	JCRB (0066)	–	n.d.	n.d.	n.d.
G361	Melanoma (skin)	JCRB (9074)	–	±	–	±
C32TG	Amelanotic melanoma (skin)	JCRB (0227)	–	±	–	±
MKN45	Adenocarcinoma (stomach)	JCRB (0254)	+	n.d.	n.d.	n.d.
N-1	Normal fibroblast (skin)	Established in our laboratory	–	–	–	–

(#) JCRB, Japanese cancer reseach resources bank. The number in parentheses represents the catalog number of the cells from JCRB; *1 and *2 level of immunohistochemical expression of low-density lipoprotein receptor (LDL-R) and intensity of fluorescence from Photofrin, respectively; (++) strongly positive in all of the cells; (+) weakly positive in all of the cells; (±) weakly positive in some (less than 50%) of the cells; (–) negative in all of the cells; n.d., not determined.

adenocarcinoma (MKN45) cell lines were significantly lower at 2.5 J/cm^2 compared to those of the melanoma lines (Mewo, G361, and C32TG). Both Mewo and G361 were highly melanin-producing cells, whereas C32TG cells produced little amount of melanin. Since survivals of these three melanoma lines were comparable, the amount of melanin did not affect the susceptibility to the present protocol of Photofrin-PDT. In the normal fibroblast cell line, N-1, Photofrin-PDT exerted a modest lytic effect and their sensitivity was comparable to that of Mewo. On the contrary, survivals were more than 95% in all of the cell lines tested after laser irradiation without Photofrin pre-treatment. The representative data of HSC-2, Mewo and N-1 are depicted in Fig. 1.

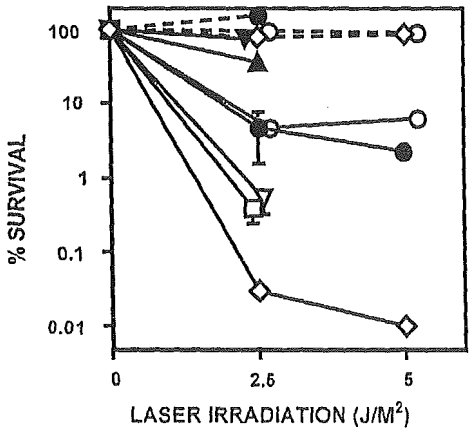

Fig. 1 Post-Photofrin-PDT survivals in human tumor cell lines. HSC-2 (◇), HSC-3 (□) MKN45 (▽), Mewo (●), G361 (▼) and C32TG (▲) cells and N-1 (○) as a control were treated with Photofrin and subsequently exposed to laser and cell survivals were examined (solid lines). Survivals of HSC-2 (◇), Mewo (●) and N-1 (○) cells without Photofrin treatment were also depicted with dashed lines. Each point represents an average of four dishes. Vertical bars represent the mean ± S.D. In most of the points, the S.D.s are smaller than the symbols.

In this study, we demonstrated that SCC and adenocarcinoma cells were more susceptible than melanoma lines. It has been postulated that melanin is one of the factors that account for the resistance of melanoma cells to the Photofrin-PDT, because this molecules not only protects the intracellular organelles from the visible light but also scavenges Photofrin-PDT-induced ROS, dampering cellular damages by PDT. However, the present study showed no difference in cell survival after Photofrin-PDT between melanotic and amelanotic melanoma cells. This observation suggested that the amount of melanin in the cells did not affect the sensitivity to killing by PDT. On the other hand, both melanotic and nonmelanotic melanoma cells were found to minimally express LDL-R. The expression of LDL-R in SCC and adenocarcinoma cells was higher than melanoma cells. By fluorescence microscopy, the uptake of Photofrin was high in the cells with strong expression of LDL-R, while low LDL-R expression was correlated with minimal incorporation of Photofrin. Furthermore, Photofrin fluorescence was barely observed in the presence of LDL, not HDL, implying that exogenous LDL occupied LDL-R and did not enable Photofrin to access them. These data confirm that the sensitivity to Photofrin-PDT among tumors depends on the levels of Photofrin incorporated through LDL-R. Our study demonstrated that Photofrin was easily introduced into cells with high LDL-R compared to cells with the low LDL-R expression, suggesting that Photofrin-PDT sensitivity of cells stems partly from the ability of incorporation of Photofrin through LDL-R. Our data also suggest that the efficacy of Photofrin-PDT can be predicted by examining the LDL-R expression in biopsy specimens of tumors.

References

[1] Dolmana D, Fukumura D, Jain PK. Photodynamic therapy for cancer. Nat Rev/Cancer 2003;3:380–7.
[2] Dougherty TJ, Gomer CJ, Henderson BW, Jori G, Kessel D, Korberik M, Moan J, Peng Q. Photodynamic therapy; review. J Natl Cancer Inst 1998;90:889–905.
[3] Korbelik M, Krosl G. Cellular levels of photosensitizers in tumors: role of proximity to the blood supply. Br J Cancer 1994;90:604–10.
[4] Allison BA, Pritchard PH, Levy JG. Evidence for low-density lipoprotein receptor-mediated uptake of benzoporphyrin derivative. Br J Cancer 1994;69:833–9.
[5] Gal D, Mcdonald PC, Porter JC, Simpson ER. Cholesterol metabolism in cancer cells in monolayer culture. III. Low density lipoprotein metabolism. Int J Cancer 1981;28:315–9.
[6] Jori G, Reddi E. The role of lipoproteins in the delivery of tumor-targeting photosensitizers. Int J Biochem 1993;25: 1369–75.
[7] Luna M, Ferrario A, Rucker N, Gomer CJ. Decreased expression and function of α-2 macroglogulin receptor-low density lipoprotein receptor-related protein in photodynamic therapy-resistant mouse tumor cells. Cancer Res 1995;55: 820–3.
[8] Roberts WG, Berns M. In vitro photosensitization. I. Cellular uptake and subcellular localization on mono-l-aspartyl chlorin e6, chloro-aluminium sulfonated phthalocyanine, and photofrin II. Lasers Surg Med 1989;9: 90–101.
[9] Ma LW, Moan J, Steen HB, Iani V. Anti-tumor activity of photodynamic therapy in combination with mitomycin C in nude mice with human colon adenocarcinoma. Br J Cancer 1995;71:950–6.
[10] Moriwaki S, Stefanini M, Lehmann AR, Hoeijmakers JH, Robbins JH, Rapin I, Botta E, Tanganelli B, Vermeulen W, Broughton BC, Kraemer KH. DNA repair and ultraviolet mutagenesis in cells from a new patient with xeroderma pigmentosum group G and Cockayne syndrome resemble xeroderma pigmentosum cells. J Invest Dermatol 1996;107: 647–53.

Junko Misawa
Shin-Ichi Moriwaki*
Masahiro Takigawa
Department of Dermatology
Hamamatsu University School of Medicine
Hamamatsu
Japan

Shin-Ichi Moriwaki*
Eiji Kohno
Toru Hirano
Photon Medical Research Center
Hamamatsu University School of Medicine
Hamamatsu
Japan

Yoshiki Tokura
Department of Dermatology, University of Occupational and Environmental Health
Kitakyusyu
Japan
*Corresponding author. Tel.: +81 53 435 2395
fax: +81 53 435 2394
E-mail address: smori@hama-med.ac.jp
(S.-I. Moriwaki)

28 July 2004

Photodermatol Photoimmunol Photomed 2005; 21: 287–292
Blackwell Munksgaard

Photodermatology
Photoimmunology
& Photomedicine

Determination of action spectrum for sparfloxacin-photosensitized single-strand breaks in plasmid pBR322 DNA

Katsuhide Sayama[1,2], Yuki Kobayashi[2], Hitoshi Fujita[2], Atsushi Ito[3], Yoshiki Tokura[4], Masako Sasaki[2]

[1]*Nippo Electric Co. Ltd., Hiratsuka, Kanagawa, Japan,* [2]*Research Institute of Science and Technology, Tokai University, Hiratsuka, Kanagawa, Japan,* [3]*Department of Applied Science, School of Engineering, Tokai University, Hiratsuka, Kanagwa, Japan, and* [4]*Department of Dermatology, School of Medicine, University of Occupational and Environmental Health, Yahata-nishi-ku, Fukuoka, Japan*

Background: Various drugs have been reported to induce photosensitivity as a side effect. Sparfloxacin (SPFX) is well known to trigger dermatological phototoxicity upon solar radiation exposure.
Purpose: To prevent SPFX-induced phototoxicity, we determined the wavelength range responsible for SPFX phototoxicity.
Methods: The action spectrum for SPFX photosensitization was assessed by the formation of single-strand breaks in plasmid pBR322 DNA.
Results: The wavelengths of light leading to the formation of single-strand breaks were in the ultraviolet A (UVA) and visible ranges. In comparison with the absorption spectrum, we found that SPFX absorption primarily contributed to the action spectrum of single-strand break formation, but it even expanded to the visible range (between 320 and 480 nm) beyond the absorption wavelengths.
Conclusion: The findings suggest that protection of skin from short wavelengths of visible light beyond the absorption wavelengths as well as UVA light is of primary importance in prevention against induction of SPFX phototoxicity.

Key words: action spectrum; photoprotection; photosensitization; plasmid DNA; single-strand breaks; sparfloxacin.

A wide variety of new synthetic drugs have been developed to apply to clinical treatments. However, because of the frequent use of these drugs in aged populations, drug-induced photosensitivity has been a serious problem as a side effect. Fluoroquinolone antibacterial agents are known to be typical photosensitive drugs (1, 2). Both phototoxicity and photoallergy play a role in the pathogenesis of fluoroquinolone photosensitivity (2, 3), depending on their chemical structures (2). The phototoxic property has been reported to be determined at least partly by a substituent at the 8-position of the structural backbone (2, 4). In an animal model, reactive oxygen species are involved in the phototoxicity (5). Other accumulated literatures on fluoroquinolne phototoxicity in clinical and laboratory studies have been reviewed (6). Among fluoroquinolones, sparfloxacin (SPFX) has been reported to cause a high incidence of photosensitivity, which has been shown to be phototoxic but not photoallergic reactions (1, 2, 7–9).

The fundamental way to prevent this side effect is photoprotection of skin from its action spectrum. While it is not easy to determine the action spectrum of a given phototoxic drug by using the cutaneous response, its *in vitro* phototoxicity can be assessed easily and quantitatively by detecting the photosensitized formation of plasmid DNA strand breaks (7, 10–14). *In vitro* photochemical studies on SPFX phototoxicity have mainly focused on plasmid DNA strand breakage (7, 10, 14). The induction of DNA strand breakage by SPFX has been shown to relate to singlet oxygen molecules generated by SPFX photoexcitation (10). A possible involvement of DNA damage in SPFX phototoxicity is suggested by the accumulation of SPFX in the nuclei of human buccal mucosa cells (15).

In this study, we used the *in vitro* DNA strand-breaking activity as a useful indicator of SPFX phototoxicity. The results demonstrate that the action spectrum for SPFX photosensitized formation of single-strand breaks in plasmid pBR322 DNA

encompasses from the ultraviolet A (UVA) to the short wavelength range of visible light.

Materials and methods

Materials

Plasmid pBR322 DNA was a product of MBI Fermentas (Vilnius, Lithuania). SPFX [CAS: 110871-86-8] was kindly provided by Dainippon Pharmaceutical Co. Ltd. (Osaka, Japan). The structural formula is shown in Fig. 1. Agarose ME was purchased from Iwai Chemicals Company Ltd. (Tokyo, Japan). Ethidium bromide was from Nippon Gene Co., Ltd. (Tokyo, Japan), and Tris was from Sigma Chemical Co. (St. Louis, MO, USA). Tris-HCl, EDTA·2Na, bromophenol blue, glycerol, and 5 × TBE buffer (89 mM Tris, 89 mM boric acid, and 2 mM EDTA; pH 8.3) were from Wako Pure Chemical Industries, Ltd. (Osaka, Japan).

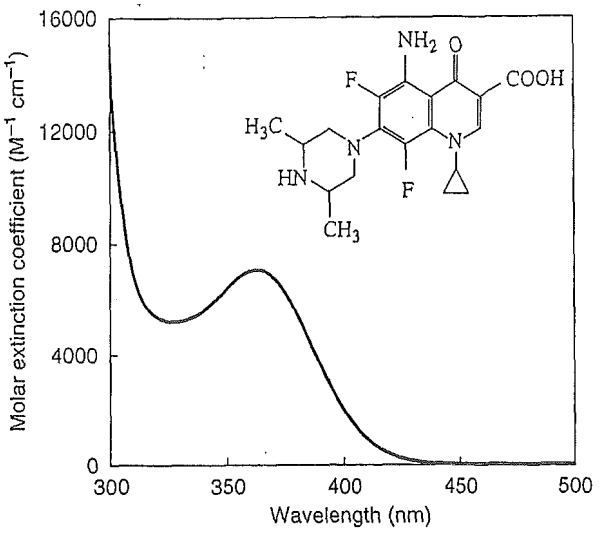

Fig. 1. Absorption spectrum of sparfloxacin (SPFX) (concentration: 50 μM) in TE buffer, containing 0.4% dimethylformamide, and the structural formula of SPFX.

Absorption spectrum of SPFX

SPFX was dissolved in TE buffer (10 mM Tris-HCl, 1 mM EDTA·2Na, pH 8.0) containing 0.4% *N,N*-dimethylformamide (DMF). DMF was added to solubilize SPFX in TE buffer. The concentration of SPFX was 50 μM. The absorption spectrum of SPFX was measured with a spectrophotometer (Model MPS-2000, Shimadzu Co., Kyoto, Japan) at 25 ± 0.5 °C.

UVA irradiation with BLB lamps

The sample solution containing plasmid pBR322 DNA and SPFX prepared in TE buffer was irradiated with BLB lamps to measure the UVA fluence dependence of single-strand breaks. The final concentrations of the DNA and SPFX were 5.55 μg/ml and 3.5 μM, respectively. A glass capillary (Drummond Scientific Co., Broomall, PA, USA) was filled with the solution (10 μl). Note that the glass does not absorb in UVA light. The temperature of the solution was maintained at 25 °C throughout the course of UVA irradiation. Irradiation of the solution was performed with two BLB lamp tubes arranged in parallel (Nominal lamp power: 32 W, specially manufactured by Nippo Electric Co, Ltd., Kanagawa, Japan) under air-saturated conditions. The lamp had a 300–420 nm emission range with the maximum at 350 nm. The UVA irradiance was measured with a UV radiometer (Model UVR-36, Topcon Co., Tokyo, Japan) to be 30 or 50 W/m^2.

Monochromatic light irradiation

To measure the action spectrum for formation of single-strand breaks, the sample solution (10 μl) in the same type of capillary as described above was irradiated with monochromatic light at different wavelengths from 320 to 480 nm. The solution contained the plasmid DNA (5.55 μg/ml) and SPFX (10 μM) dissolved in TE buffer. Monochromatic light irradiation of the sample was performed by means of a 'spectroirradiator' (Model MLS-121, ORC MANUFACTURING CO, LTD., Tokyo, Japan). The apparatus used consists of a 1 kW xenon short arc lamp optically coupled to a single grating monochromator. The three capillaries were fixed with a holder set on the exit of the monochromator in parallel, and uniformly irradiated with monochromatic light at room temperature under air-saturated conditions. The apparatus was set to irradiate monochromatic light at 320, 326, 340, 360, 375, 400, 440 and 480 nm, respectively. The spectral resolution was 4 nm. Several kinds of cut-off filters were used to reduce shorter wavelengths of scattered light for the longer wavelength monochromatic light. The values of irradiance were measured with an IL1745 UV Curing Radiometer System (International light Inc, Newburyport, MA, USA), as 17 W/m^2 (320 nm), 21 W/m^2 (326 nm), 32 W/m^2 (340 nm), 48 W/m^2 (360 nm), 60 W/m^2 (375 nm), 79 W/m^2 (400 nm), 44 W/m^2 (440 nm) and 48 W/m^2 (480 nm).

Agarose gel electrophoresis

Separation of the different forms of plasmid pBR322 DNA, i.e., the closed circular form (native conformation), the open circular form (resulting from single-strand breaks) and the linear form (resulting from double-strand breaks), was performed by horizontal agarose gel electrophoresis (1.1% agarose slab gels) in TBE buffer. The irradiated solution (2 μl) was mixed

ith 1 µl of loading buffer (0.25% bromophenol blue, 0% glycerol in TBE buffer). The mixed solution was pplied to wells in the slab and electrophoresed with a Aupid-3 system (Cosmo Bio Co., Ltd., Tokyo, Japan) or 40 min at 100 V. After electrophoresis, the gels vere stained with ethidium bromide (0.5 µg/ml) for 0 min and rinsed with 0.5 × TBE buffer for 5 min. The DNA forms that were separated by electrophoresis were visualized by fluorescence of ethidium bromide, which was intercalated with the DNA forms, on a transilluminator (Model TFP-10 M, Vilber Lournat, Marne-La-Vallée Cedex, France). The fluorescent patterns were photographed on a Polaroid-type 667 positive film through a red filter. The resulting photographs were scanned into a computer and processed using Scion Image program (Scion Co., Frederick, MD, USA). The ratios of the relative amounts of the open circular form to the closed circular form were calculated from the peak areas of the densitometric trace of the fluorescence image. In addition, as the fluorescence intensity of ethidium bromide bound to the closed circular form was less than that bound to the open circular form by a factor of 1.42 (16), amounts of the closed circular form were corrected by this factor.

Results

Absorption spectrum of SPFX

The absorption spectrum of SPFX in TE buffer containing 0.4% DMF was measured as shown in Fig. 1. SPFX had an absorption band in the range of 320–450 nm, with a peak at 362 nm. The molar extinction coefficient at the absorption maximum was 7100 $M^{-1} cm^{-1}$.

DNA strand-breaking activity of UVA irradiation with SPFX

The DNA strand-breaking activity of photosensitized SPFX was identified by 1.1% agarose gel electrophoretic separation of the DNA forms after irradiation with the BLB lamps for 20 min, 40 or 60 min. When the plasmid DNA was irradiated in the presence of SPFX, single-strand breaks in the DNA were produced, converting the closed circular form into the open circular form (Fig. 2). The fluorescence intensities of ethidium bromide in the electrophoretic bands depend on the concentrations of the DNA forms. The photocleavage efficiency was increased with increasing UVA-irradiated fluence (Fig. 3). The amount of the closed circular form decreased exponentially with increasing fluence, whereas the amount of the open circular form increased conversely. To analyze these data using the hit theory, the values of

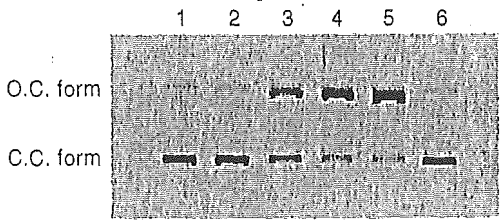

Fig. 2. Electrophoretic patterns on 1.1% agarose gel showing single-strand breaks in plasmid pBR322 DNA by sparfloxacin (SPFX) photosensitization. Concentration of SPFX, 3.5 µM; light source, BLB lamps; irradiance, 50 W/m^2. C.C., closed circular; O.C., open circular; lane 1, dark control (−SPFX); lane 2, dark control (+SPFX); lane 3, fluence 60 kJ/m^2 (+SPFX); lane 4, fluence 120 kJ/m^2 (+SPFX); lane 5, fluence 180 kJ/m^2 (+SPFX); lane 6, fluence 180 kJ/m^2 (−SPFX).

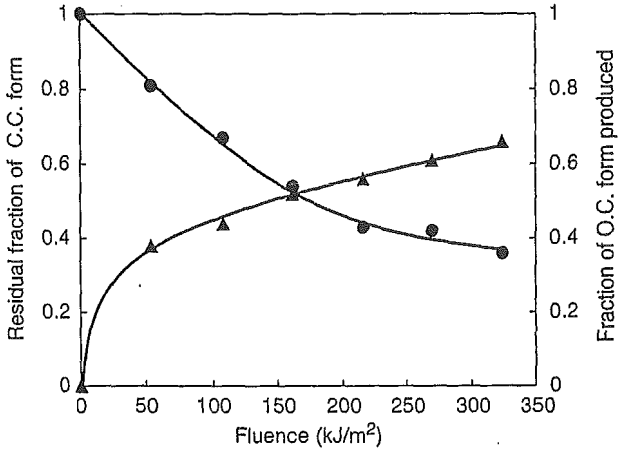

Fig. 3. Change of residual fraction of CC form and fraction of OC form produced with increasing fluence. Concentration of sparfloxacin, 3.5 µM; light source: BLB lamps; irradiance, 30 W/m^2; C.C., closed circular (●); O.C., open circular (▲).

−*ln* (fraction of closed circular form) were plotted as a function of UVA-irradiated fluence. As shown in Fig. 4, the change in the residual fraction of the closed circular form fitted to the single-hit kinetics in the range of 0–162 kJ/m^2. No significant electrophoretic band corresponding to the linear form resulting from double-strand breaks was observed in the irradiated fluence range examined. As a dark control experiment, an unirradiated mixture of the DNA and SPFX was also analyzed electrophoretically. The closed circular form in the mixture migrated at the same rate as the DNA in the absence of SPFX, showing that no electrophoretically detectable modification of the DNA was induced by addition of SPFX in the dark (dark control). Irradiation of the DNA in the absence of SPFX (irradiated control) did not alter the electrophoretic

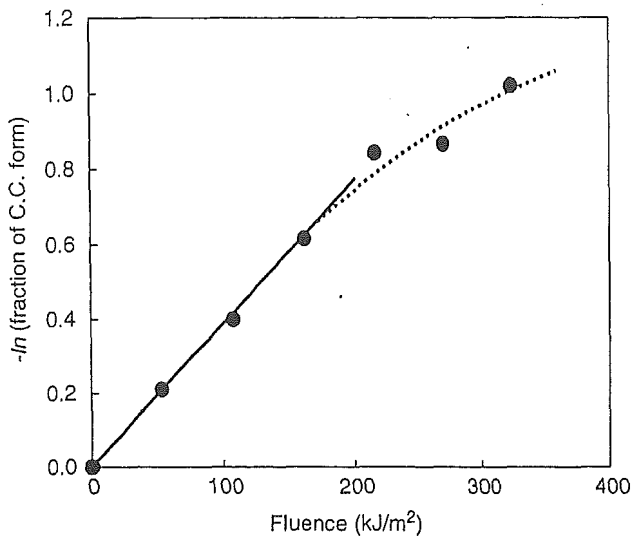

Fig. 4. Fluence dependence of the photosensitized single-strand breaks. Concentration of sparfloxacin: 3.5 μM, Light source, BLB lamps; Irradiance, 30 W/m^2; C.C., closed circular.

pattern under the present experimental conditions. These findings indicate that SPFX can behave as a UVA photosensitizer for induction of the photosensitized formation of strand breakage in the DNA.

Action spectrum for the SPFX-photosensitized formation of single-strand breaks

The action spectrum for the SPFX-photosensitized formation of single-strand breaks was determined for the 320–480 nm range. As mentioned above, the lesion in the range of a low fluence was recognized to follow the single-hit kinetics with respect to the fluence. This relation was reconfirmed in cases of monochromatic irradiation (Fig. 5). The lines illustrated in the figure indicate best linear regressions constrained through the origin. The result enabled us to compute the action cross-section of the photocleavage caused by irradiations at different wavelengths. The data were obtained after the correction with respect to the irradiated control experiment. Consequently, the action spectrum for the SPFX-photosensitized formation of single-strand breaks was determined as shown in Fig. 6. The maximum response was observed at around 370 nm. As illustrated, the maximum response shifted slightly to longer wavelengths when compared with the absorption spectrum. In addition, extension of the action spectrum to the visible region beyond the absorption wavelengths was apparent.

Discussion

We presented the action spectrum for the *in vitro* formation of single-strand breaks in plasmid pBR322

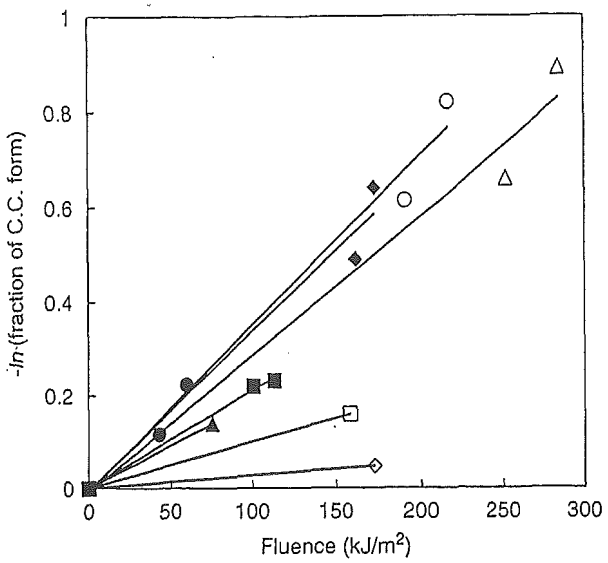

Fig. 5. Fluence dependence of the photosensitized single-strand breaks by irradiation with monochromatic lights. Concentration of sparfloxacin, 10 μM; Light source, the xenon short arc lamp; C.C., closed circular; ●, 320 nm; ▲, 326 nm; ■, 340 nm; ◆, 360 nm; ○, 375 nm; △, 400 nm; □, 440 nm; ◇, 480 nm.

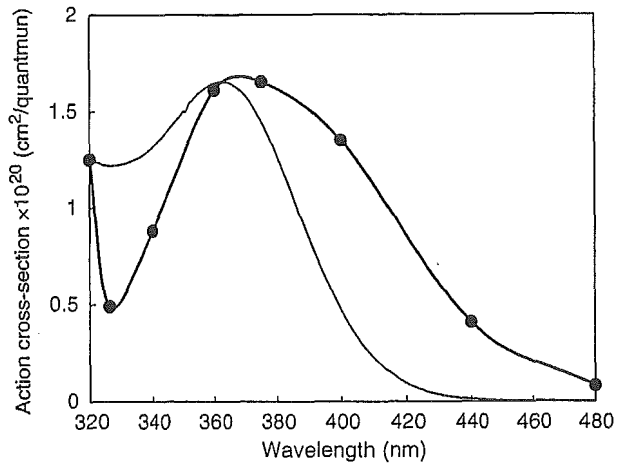

Fig. 6. Action spectrum for the photosensitized single-strand breaks. The spectrum was superimposed on the relative absorption spectrum of sparfloxacin. (—●—), action spectrum; (——), absorption spectrum.

DNA by photosensitization with SPFX. The action spectrum was largely reflective of the absorption spectrum. The major wavelengths were in the UVA range, but visible light beyond the absorption wavelengths was also found to be involved in the formation of single-strand breaks in the plasmid DNA. The present result has a clinical meaning in selection of the wavelength range of light to be blocked for prevention of SPFX-induced phototoxicity.

A key point of the action spectrum obtained in the resent study is the extension to visible range beyond ıe absorption wavelengths. It has been shown that at ;ast three photoproducts are generated by irradiation f SPFX with UV light from a high-pressure Hg ischarge lamp (17). Although their absorption charcteristics are not known, it is likely that the photo-)roducts are involved in the extension of the action pectrum, given that they absorb light at longer vavelengths than SPFX and form single-strand)reaks. A slight increase in the absorption of UVA-rradiated solution of SPFX alone or that of SPFX vith calf thymus DNA in the visible range beyond the absorption wavelengths may be a line of evidence supporting the generation of the photoproducts (data not shown). Further work has to be carried out to resolve the cause of the extension. Although photoaugmentation with UVA and UVB has been shown to trigger SPFX phototoxicity (7), it is suggested that visible light has also been implied as an inducer of SPFX phototoxicity on the basis of its action spectrum. Occurrence of strand breakage observed by irradiation with a commonly used fluorescent lamp with a broad visible emission spectrum supports the present findings (7).

The induction mechanisms of SPFX-photosensitized DNA damage have been studied in some papers. For example, plasmid DNA strand breakage caused by photosensitization with SPFX was demonstrated to be mainly a TypeII photosensitized reaction (10), while singlet oxygen molecules generally do not induce direct strand breakage both within isolated and cellular DNA (18). Involvement of hydroxyl radicals in SPFX-photosensitized oxidative damage to DNA in retinal pigment epithelial cells was also proposed (19). Photoexcited fluoroqinolones other than SPFX have been shown to react with DNA directly in addition to the generation of active oxygen species. For example, the production of cyclobutane pyrimidine dimers through the triplet energy transfer mechanism upon UVA excitation (20), and a possible involvement of carbene intermediates in DNA strand breakage (13, 21), were shown. Thus, it is most likely that photosensitized DNA damage in the presence of SPFX occurs by way of a variety of mechanisms.

We have assessed quantitatively the preventive abilities of conventional clothes and commercial sunscreens against SPFX phototoxicity, referring to the photosensitized strand breakage in the plasmid DNA *in vitro* (22, 23). The present study supported the validity of adopting SPFX-photosensitized strand breakage as an indicator of UVA protection.

Acknowledgements

This study was partly supported by a Grant-in-Aid from the General Research Organization of Tokai University (RP-8, 2002). We thank Dainippon Pharmaceutical Co., Ltd. for their kind supply of sparfloxacin, and we also thank Dr. Itsuro Matsuo for his valuable comments and thoughtful discussion.

References

1. Domagala JM. Structure–activity and structure–side-effect relationship for the quinolone antibacterials. J Antimicrobial Chemotherapy 1994; 33: 685–706.
2. Tokura Y. Quinolone photoallergy: photosensitivity dermatitis induced by systemic administration of photohaptenic drugs. J Dermatol Sci 1998; 18: 1–10.
3. Horio T, Miyauchi H, Asada Y, Aoki Y, Harada M. Phototoxicity and photoallergenicity of quinolones in guinea pigs. J Dermatol Sci 1994; 7: 130–135.
4. Yabe K, Goto K, Jinbo T, Sekiguchi M, Furuhama K. Structure-phototoxicity relationship in Balb/c mice treated with fluoroquinolone derivatives, followed by ultraviolet-A irradiation. Toxicol Lett 2005; 157: 203–210.
5. Wagai N, Tawara K. Important role of oxygen metabolites in quinolone antibacterial agent-induced cutaneous phototoxicity in mice. Arch Toxicol 1991; 65: 495–499.
6. Man I, Traynor NJ, Ferguson J. Recent developments in fluoroquinolone phototoxicity. Photodermatol Photoimmunol Photomedicine 1999; 15: 32–33.
7. Tokura Y, Iwamoto Y, Mizutani K, Takigawa M. Sparfloxacin phototoxicity: potential photoaugmentation by ultraviolet A and B sources. Arch Dermatol Res 1996; 288: 45–50.
8. Hamanaka H, Mizutani H, Asahig K, Shimizu M. Melanocyte melanin augments sparfloxacin-induced phototoxicity. J Dermatol Sci 1999; 21: 27–33.
9. Schentag JJ. Sparfloxacin: a review. Clin Ther 2000; 22: 372–387.
10. Umezawa N, Arakane K, Ryu A, Mashiko S, Hirobe M, Nagano T. Participation of reactive oxygen species in phototoxicity induced by quinolone antibacterial agents. Arch Biochem Biophys 1997; 342: 275–281.
11. Iwamoto Y, Itoyama T, Yasuda K, et al. Photodynamic deoxyribonucleic acid (DNA) strand breaking activity of enoxacin and afloqualone. Chem Pharm Bull 1992; 40: 1868–1870.
12. Iwamoto Y, Kurita A, Shimizu T, et al. DNA strand-breaking activities of quinolone antimicrobial agents under visible light irradiation. Biol Pharm Bull 1994; 17: 654–657.
13. Sortino S, Condorelli G, De Guidi G, Giuffrida S. Molecular mechanism of photosensitization XI. Membrane damage and DNA cleavage photoinduced by enoxacin. Photochem Photobiol 1998; 68: 652–659.
14. Yamamoto Y, Tsurumaki Y, Takei M, Hosaka M, Oomori Y. In vitro method for prediction of the phototoxic potentials of fluoroquinolones. Toxicol In Vitro 2001; 15: 721–727.
15. Sayama K, Morishima A, Fujita H, Ito A, Nakamura K, Sasaki M. Possible targets of sparfloxacin-photosensitization in human buccal mucosa cells as revealed by fluorescence microscopy and microspectrofluorometry. J Photopolymer Sci Tech 2003; 16: 655–660.
16. Lloyd RS, Haidle CW, Robberson DL. Bleomycin-fragmentation of double-stranded DNA. Biochemistry 1978; 17: 1890–1896.
17. Engler M, Rüsing G, Sörgel F, Holzgrabe U. Defluorinated sparfloxacin as a new photoproduct identified by liquid

chromatography coupled with UV detection and tandem mass spectrometry. Antimicrobial Agents Chemother 1998; 42: 1151–1159.
18. Ravanat J, Sauvaigo S, Caillat S, et al. Singlet oxygen-mediated damage to cellular DNA determined by the comet assay associated with DNA repair enzymes. Biol Chem 2004; 385: 17–20.
19. Verna LK, Holman SA, Lee VC, Hoh J. UVA-induced oxidative damage in retinal pigment epithelial cells after H_2O_2 or sparfloxacin exporsure. Cell Biol Toxicol 2000; 16: 303–312.
20. Sauvaigo S, Douki T, Odin F, Caillat S, Ravanat J, Cadet J. Analysis of fluoroquinolone-mediated photosensitization of 2′-deoxyguanosine, calf thymus and cellular DNA: determination of type-I, type-II and triplet-triplet energy transfer mechanism contribution. Photochem Photobiol 2001; 73: 230–237.
21. Martinez LJ, Li G, Chignell CF. Photogeneration of fluoride by the fluoroquinolone antimicrobial agents lomefloxacin and fleroxacin. Photochem Photobiol 1997; 65: 599–602.
22. Sayama K, Ishikawa K, Yamada R, Fujita H, Ito A, Sasaki M. In vitro evaluation of preventive ability of commercial sunscreens against induction of photosensitivity with sparfloxacin. Photomed Photobiol 2002; 24: 43–46.
23. Sasaki M, Mishima E, Kagami Y, Saito M. Studies on protection of the human body from UV radiation-Transmittance and reflectance of UV by white fabric-. Proceedings of 25th session of the CIE, -San Diego, -25 June–2 July, CIE Central Bureau, Vienna, 2003, D6-53-D6-54.

Accepted for publication 14 September 2005

Corresponding author:
Katsuhide Sayama
Research Institute of Science and Technology
Tokai University
1117 Kitakaname
Hiratsuka
Kanagawa 259-1292
Japan
Tel: +81-463-58-1211
Fax: +81-463-58-1203
e-mail: sayama-07@theia.ocn.ne.jp

Journal of Dermatological Science (2006) 41, 127–136

ELSEVIER

Journal of Dermatological SCIENCE

www.intl.elsevierhealth.com/journals/jods

Establishment of murine model of allergic photocontact dermatitis to ketoprofen and characterization of pathogenic T cells

Satoshi Imai [a,b], Kenji Atarashi [a,b], Koichi Ikesue [b], Katsuhiko Akiyama [b], Yoshiki Tokura [a,*]

[a] *Department of Dermatology, University of Occupational and Environmental Health, 1-1 Iseigaoka, Yahatanishi-ku, Kitakyushu 807-8555, Japan*
[b] *Fundamental Research Laboratories, Hisamitsu Pharmaceutical Co. Inc., Tsukuba, Japan*

Received 9 June 2005; received in revised form 17 August 2005; accepted 26 August 2005

KEYWORDS
Photocontact dermatitis;
Contact photoallergy;
Ketoprofen;
Chemokine

Summary

Background: Ketoprofen is well known to evoke the allergic type of photocontact dermatitis when it is applied to the skin and irradiated with ultraviolet A (UVA) light.
Objective: We aimed to establish a murine model of this photosensitivity and to characterize pathogenic T cells concerned with the sensitivity.
Methods: Various strains of mice were sensitized on two consecutive days by application of ketoprofen to the shaved abdomen and irradiation of the skin with UVA. Five days later, they were elicited with ketoprofen plus UVA on the earlobes. Immune lymph node cells and epidermal cells from the challenged sites were analyzed by RT-PCR.
Results: Mice were successfully sensitized and challenged with 4% and 2% ketoprofen, respective, plus UVA at20 J/cm^2. The responses in H-2^k mice were higher than those in the other strains examined. Immune lymph node CD4$^+$ or CD8$^+$ cells from ketoprofen-photosensitized H-2^k mice were transferred i.v. to naïve syngeneic recipients. Mice receiving CD4$^+$ but not CD8$^+$ cells exhibited ketoprofen photosensitivity, but transference of both CD4$^+$ and CD8$^+$ cell populations was more effective. Lymph node cells from photosensitized mice expressed high levels of mRNA for Th2 cytokine (IL-4) and Th2 chemokine receptor (CCR4) as well as Th1 cytokine (IFN-γ) and Th1 chemokine receptor (CXCR3), as assessed by RT-PCR. In addition, epidermal cells from challenged earlobes expressed increased levels of both Th1 (TARC) and Th2 (Mig) chemokines.
Conclusion: It is considered that not only Th1 but also Th2 cells participate in the pathogenesis of murine photocontact dermatitis to ketoprofen.

* Corresponding author. Tel.: +81 93 691 7445; fax: +81 93 691 0907.
E-mail address: tokura@med.uoeh-u.ac.jp (Y. Tokura).

0923-1811/$30.00
doi:10.1016/j.jdermsci.2005.08.006

1. Introduction

Photocontact dermatitis is a specialized form of contact dermatitis evoked by various chemicals, such as halogenated salicylanilides, musk ambrette, benzophenone-3 (oxybenzone), and non-steroidal anti-inflammatory drugs [1]. Patients develop dermatitis, when their skin is exposed to these agents and subsequent ultraviolet (UV) light. This disorder is pathohysiologically divided into two types, phototoxic and photoallergic ones. While the phototoxic dermatitis is mediated by oxygen intermediates, the photoallergic type, also known as contact photosensitivity, is a well-organized cutaneous sensitivity that is immunologically induced and elicited with photoallergic agent and UVA. Recently, the incidence of the photoallergic type is higher than the phototoxic one, because the major causative agents are non-steroidal anti-inflammatory drug with photoallergic properties [2].

It has been clarified that the majority of photoallergic agents are photohaptens, which bind covalently to protein via the formation of free radicals resulting from UV irradiation [2]. Because of this photobinding ability, cells are easily photomodified with photohapten under exposure to UVA, which is the action spectrum of photocontact dermatitis. The main sequential events in photocontact dermatitis have been investigated with 3,3′,4′,5-tetrachlorosalicylanilide (TCSA) in mice [3,4] and are virtually the same as those of ordinary contact dermatitis except for the requirement of UV irradiation in sensitization and challenge. Photoconjugation of epidermal cells with TCSA is the initial step. Langerhans cells (LC), which are professional antigen-presenting cells in the epidermis, play an important role. Photohapten-bearing LC migrates to draining lymph nodes in the sensitization phase [5]. T cells sensitized by photohapten-bearing LC induce the photosensitivity [3] and suppressor or regulatory T cells involved in this sensitivity have been identified [6].

Ketoprofen (KP), widely used as a topical non-steroidal anti-inflammatory drug, is clinically well known to induce the allergic type of photocontact dermatitis [7–11]. In addition to the high incidence of occurrence of photocontact dermatitis, KP is an interesting drug in its cross-photoreactivity with thiaprofenic acid, suprofen, phenofibrate, and benzophenone-3 [7–11]. These substances have a photohaptenic moiety [2] as well as a phototoxic ability [12,13].

A model of KP photocontact dermatitis has been reported using guinea pigs [11]. However, little is known regarding the immunological characteristics of photocontact dermatitis to KP. In this study, we established a murine model of KP photosensitivity and investigated the immunological mechanism, focusing on the involvement of Th1 and Th2 cells.

2. Materials and methods

2.1. Animals

AKR/N (H-2^k), CBA/J (H-2^k), C3H/He (H-2^k), BALB/c (H-2^d), DBA/2 (H-2^d), A/J (H-2^a), C57BL/6 (B6; H-2^b) were obtained from Kyudo Co. Ltd. (Kumamoto, Japan). BALB.K/Ola (H-2^k) mice were kindly provided by National Institute of Genetics (Mishima, Japan). Female mice, 8-week old, were used in this study.

2.2. Chemicals

KP was obtained from Hisamitsu Pharmaceutical Co. Inc. (Tokyo, Japan) and 3,3′,4′,5-tetrachlorosalicylanilide (TCSA) was purchased from Kanto Chemical Co. Inc. (Tokyo, Japan).

2.3. Light source

Black light (FL20SBL-B) emitting UVA ranging from 320 to 400 nm with a peak emission at 365 nm was purchased from Toshiba Electric Co. (Tokyo, Japan). With a UV radiometer (Topcon Technohouse Corp., Tokyo, Japan), the energy output of three 20 W tubes of black light at a distance of 20 cm was 2.4 mW/cm^2 at 365 nm and 0.17 mW/cm^2 at 305 nm.

2.4. Photosensitization and photochallenge to KP

The basic method for photosesitization and photochallenge was described previously [3,4]. Mice were painted with 50 μl of 1, 2 or 4% KP in acetone to the clipped abdomen. Within 30 min, the painted site was irradiated with three tubes of black light at a distance of 20 cm for 2.5 h (20 J/cm^2 at 365 nm) unless otherwise mentioned by placing cages containing mice over the lights. We used a pane of window glass 3 mm thick to insure that no radiation below 320 nm reached the skin. The painting plus irradiation was performed on two consecutive days, i.e., days 0 and 1. Before challenge, the basal line thickness of both ears on all mice was measured with a dial thickness gauge. On day 5, all mice were challenged on both sides of each earlobe with 25 μl of 2% KP in ethanol unless otherwise described. Within 30 min, the mice received irradiation under black light at a distance of 20 cm at 20 J/cm^2 at

365 nm. Ear thickness was measured 24 h after irradiation and was expressed as the mean increment in thickness above basal line control value.

2.5. Preparation of single cell suspension of lymph node cells (LNC) and epidermal cells

Axillary and inguinal lymph nodes were collected on day 3 or 5 from mice photosensitized with KP on days 0 and 1. Single cell suspensions were prepared by teasing lymph nodes. For preparation of epidermal cells, excised murine earlobes were incubated in 0.2% trypsin. Epidermal cells were dispersed and washed three times in PBS, as described previously [14].

2.6. Adoptive transfer of sensitivity with immune LNC

Immune LNC were prepared on day 5 from KP-photosensitized AKR/N mice. To obtain purified $CD4^+$ or $CD8^+$ T cells, LNC were incubated with anti-CD4 or anti-CD8 monoclonal antibody (mAb)-conjugated magnetic beads (Dynal Inc., Oslo, Norway) and the bound cells were detached from the beads with Detachabeads (Dynal Inc.) according to the manufacture's directions. Unfractionated LNC (2×10^7 cells/mouse) or varying ratios of $CD4^+$ or $CD8^+$ T cells in 0.4 ml of phosphate buffered saline (PBS; pH 7.4) were injected i.v. into naïve recipients. The control mice were injected with PBS alone. Within 1 h after cell transfer, the recipient and control mice were challenged on the ears with 2% KP plus 20 J/cm^2 UVA, and ear swelling response was measured after 24 h. In a comparison, BALB/c mice were sensitized with 1% TCSA plus 12 J/cm^2 UVA on days 0 and 1, as described previously [3,4], and LNC were transferred to naïve syngeneic mice. Epicutaneous sensitization and challenge with TCSA plus UVA was reported [3].

2.7. Reverse transcription-polymerase chain reaction (RT-PCR) assay

Total RNA was extracted from LNC or epidermal cells using the SVTotal RNA Isolation system (Promega Co., Madison, WI, USA). To prepare first strand cDNA, 1 μg of RNA was incubated in 100 μl of buffer containing 10 mM dithiothreitol, 2.5 mM $MgCl_2$, dNTP mix, 200 U of reverse transcriptase II (Invitorogen, Carlsbad, CA, USA) and 0.1 mM oligo $(dT)_{12-18}$ (Invitorogen). Each cDNA were amplified in a 50 μl PCR solution containing 0.8 mM $MgCl_2$, dNTP mix and DNA polymerase (Roche Applied Science, Penzberg, Germany) with synthesized primers. Samples were heated to 95 °C for 2 min, 55 °C for 2 min and 72 °C for 3 min, and cycled 40 times through 95 °C for 1 min, 55 °C for 2 min and 72 °C for 3 min. The final incubation was 72 °C for 7 min. The mixture was subjected to 1% agarose gel for electrophoresis with the indicated markers and primers for the internal standard β-actin. Each sample was applied more than two lanes in the same gel. The agarose gel was stained with ethidium bromide and photographed with UV transillumination.

The sense/antisense primer sequences were as follows. Interferon-γ (IFN-γ): 5′-TGA ACG CTA CAC ACT GCA TCT TGG-3′ and 5′-CGA CTC CTT TTC CGC TTC CTG AG-3′; IL-4: 5′-ATG GGT CTC AAC CCC CAG CTA GT-3′ and 5′-GCT CTT TAG GCT TTC CAG GAA GTC-3′; CXCR3: 5′-GCC GAT GTT CTG CTG GTG TTA A-3′ and 5′-TTT TCG ACC ACA GTT GCG GGC-3′ CCR4: 5′-TCG GAT TTG CTG TTC GTC CTG T-3′ and 5′-TAA GGC AGC AGT GAA TGA AGC C-3′; IP-10; 5′-CGC ACC TCC ACA TAG CTT ACA G-3′ and 5′-CCT ATC CTG CCC ACG TGT TGA G-3′; Mig: 5′-TGA TAA GGA ATG CAC GAT GCT C-3′ and 5′-TTC CTT GAA CGA CGA CGA CTT T-3′; TARC: 5′-CAG GAA GTT GGT GAG CTG GTA TAA-3′ and 5′-TTG TGT TCG CCT GTA GTG CAT A-3′; MDC: 5′-TCT GAT GCA GGT CCC TAT GGT-3′ and 5′-TTA TGG AGT AGC TTC TTC ACC CAG-3′; β-actin: 5′-TGG AAT CCT GTG GCA TCC ATG AAA C-3′ and 5′-TAA AAC GCA GCT CAG TAA CAG TCC G-3′.

2.8. Statistical analysis

Student's *t*-test was employed to examine the significance between the means, and $p < 0.05$ was considered statistically significant.

3. Results

3.1. Induction of photocontact dermatitis by KP plus UVA

As shown in Fig. 1, AKR/N mice were sensitized by topical painting of 4% KP and subsequent irradiation with 20 J/cm^2 UVA, or by KP alone. They were challenged on the earlobes with 2% KP and/or 20 J/cm^2 UVA. A significant ear swelling response was observed in mice challenged with both KP and UVA, whereas elicitation with KP or UVA alone did not induce the response. In mice sensitized with 4% KP alone, KP plus UVA evoked a detectable swelling response. Since elicitation with KP alone did not yield any response, this was considered to be a phototoxic response, and was significantly lower than the photoallergic response to KP. Thus, treatment with KP plus UVA was capable of inducing the allergic type of photocontact dermatitis in mice.

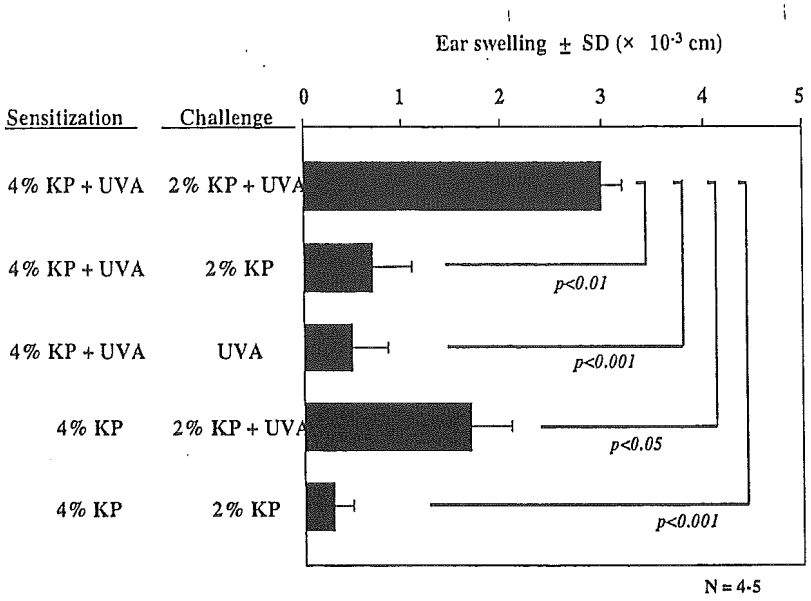

Fig. 1 Requirement of both KP and UVA for induction and elicitation of allergic photocontact dermatitis. AKR/N mice were sensitized with KP (4%) plus UVA (20 J/cm^2) or KP alone on days 0 and 1. On day 5, they were challenged on both sides of each earlobe with KP (2%) and/or subsequent UVA (20 J/cm^2). Ear swelling was measured 24 h after irradiation. Each column represents the mean ± S.D.

3.2. KP concentration and UVA dose effective for induction and elicitation of photocontact dermatitis

AKR/N and C3H/He mice were sensitized with 1, 2, or 4% KP in combination with 20 J/cm^2 UVA, and challenged with 2% KP plus 20 J/cm^2 UVA (Fig. 2A). KP at both concentrations of 2 and 4% produced significant ear swelling responses, with the latter being slightly more effective than the former. When 4% KP-photosensitized mice were challenged with 1, 2, or 4% KP in combination with 20 J/cm^2 UVA, 2 and 4% KP induced comparable responses in AKR/N mice, while all three concentrations of KP produced significant responses in C3H/He (Fig. 2B). When AKR/N mice were sensitized with 4% KP alone and challenged with 2% or 4% KP plus UVA, photochallenge with 4% KP produced two-fold higher swelling than 2% KP (data not shown), indicating that the phototoxic response of 2% KP was low.

AKR/N mice were sensitized with 4% KP and l[illegible] t 10, 20, 30 or 40 mJ/cm^2, and challenged with 2% KP plus 20 mJ/cm^2 UVA (Fig. 2C). UVA at 20, 30, and 40 mJ/cm^2 yielded significant and comparable responses. Therefore, we used 4% KP for photosensitization and 2% KP for photochallenge in combination with 20 mJ/cm^2 UVA in the following experiments.

3.3. Different reactivity in photocontact dermatitis among various mouse strains

Eight strains of mice were sensitized and challenged with KP plus UVA. AKR/N, CBA/J, C3H/He, BALB.K/Ola, and A/J exhibited higher responses than did BALB/c, DBA/2 and B6 mice (Fig. 3). Considering that BALB/c and BALB.K/Ola mice are H-2-congenic strains and thus differ only at the H-2 complex, it seems that H-2^k mice are high responders in this sensitivity.

3.4. Adoptive transfer of photocontact dermatitis

Immune LNC were taken from AKR/N mice photosensitized with KP 5 days before and injected i.v. into naïve recipients, which were challenged with KP plus UVA. As positive control, a group of mice were epicutaneously sensitized and challenged in parallel. Fig. 4A shows that mice receiving 2 × 10^7 LNC exhibited a significant degree of photocontact dermatitis but to a lesser degree than the epicutaneously sensitized mice. Along with this study, immune LNC from BALB/c mice photosensitized with TCSA were transferred to naïve syngeneic recipients. They had a stronger but similarly reduced level of response as compared to the epicutaneously sensitized mice. When donor mice were treated with UVA alone, transfer of their LNC did not induce the sensitivity in recipients (Fig. 4B).

3.5. Essential and augmentative roles of CD4$^+$ and CD8$^+$ cells, respectively, in photocontact dermatitis

CD4$^+$ or CD8$^+$ T cells (5 × 10^6 cells/mouse) purified from KP-immune LNC of AKR/N mice were trans-

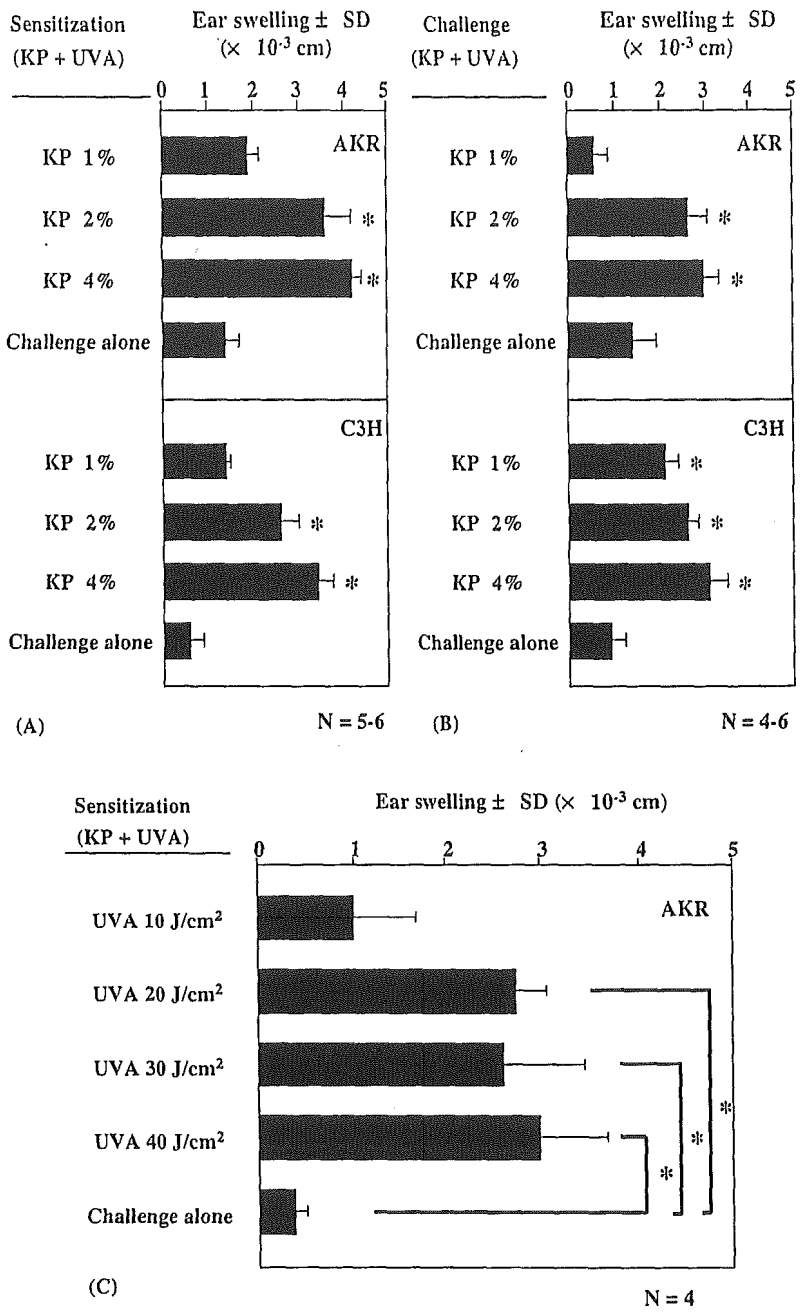

Fig. 2 Effects of KP concentration and UVA dose on sensitization and challenge of photocontact dermatitis. AKR/N and C3H/He mice were sensitized with varying doses of KP (1–4%) (A) or 4% KP (B) plus UVA (20 J/cm^2) on days 0 and 1. On day 5, they were challenged on both sides of each earlobe with 2% KP (A) or varying doses of KP (1–4%) (B) plus UVA (20 J/cm^2). In (C), AKR/N mice were sensitized with 4% KP plus varying doses (10–40 J/cm^2) of UVA and challenged with 2% KP plus 20 J/cm^2 UVA. Ear swelling was measured 24 h after irradiation. Each column represents the mean ± S.D. $^*p < 0.05$.

ferred to naïve syngeneic recipients. Upon challenge with KP plus UVA, mice injected with CD4$^+$ cells, but not CD8$^+$ or CD4$^-$CD8$^-$ cells, exhibited a significant swelling response compared to the non-injected control mice (Fig. 5). When mice were injected with increasing numbers of CD8$^+$ cells additionally with CD4$^+$ cells, 5×10^6 cells, but not 1 or 2.5×10^6 cells, enhanced the CD4$^+$ cell-induced response. This combination of CD4$^+$ and CD8$^+$ cells produced a comparable response to the epicutaneously sensitized mice. The results suggested that CD4$^+$ T cells mediate the sensitivity and CD8$^+$ T cells participate in the full responses.

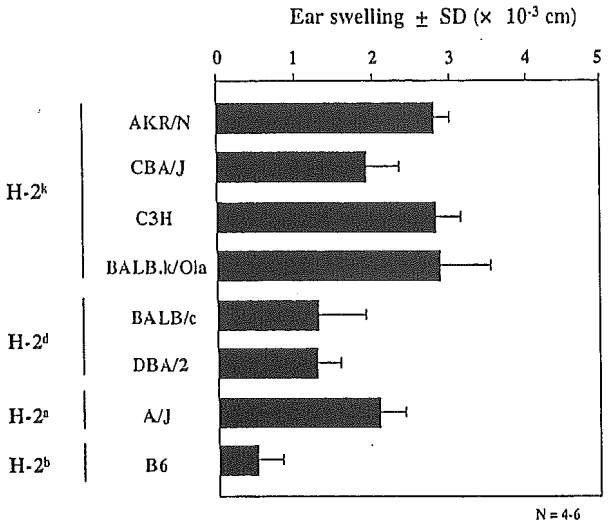

Fig. 3 Photocontact dermatitis to KP in various mouse strains with different H-2 haplotypes. Mice were sensitized with 4% KP plus 20 J/cm^2 UVA on days 0 and 1. On day 5, they were challenged with 2% KP and 20 J/cm^2 UVA. Data are expressed as: Δear swelling, representing (sensitization and challenge) – (challenge alone). Each column represents the mean ± S.D.

3.6. Elevated mRNA expression of cytokines and chemokine receptors of both Th1 and Th2 cells in immune LNC

AKR/N mice were sensitized with KP plus UVA on days 0 and 1, and single cell suspensions of immune LNC were prepared on day 1 (immediately after sensitization), 3 and 5. The expression of Th1 and Th2 cytokines, as represented by IFN-γ and IL-4, respectively, was examined by RT-PCR. As shown in Fig. 6A, KP photosensitization increased the expression of both cytokines compared to vehicle alone. Notably, IL-4 was markedly augmented by KP plus UVA on day 5.

Th1 and Th2 cells express chemokine receptor CXC chemokine receptor 3 (CXCR3) and CC chemokine receptor 4 (CCR4), respectively. The expression of these chemokine receptors was also tested in immune LNC. As most discernibly seen in day 5 LNC, CCR4 expression was remarkably enhanced by sensitization with KP plus UVA, while CXCR3 was increased to a lesser degree (Fig. 6B).

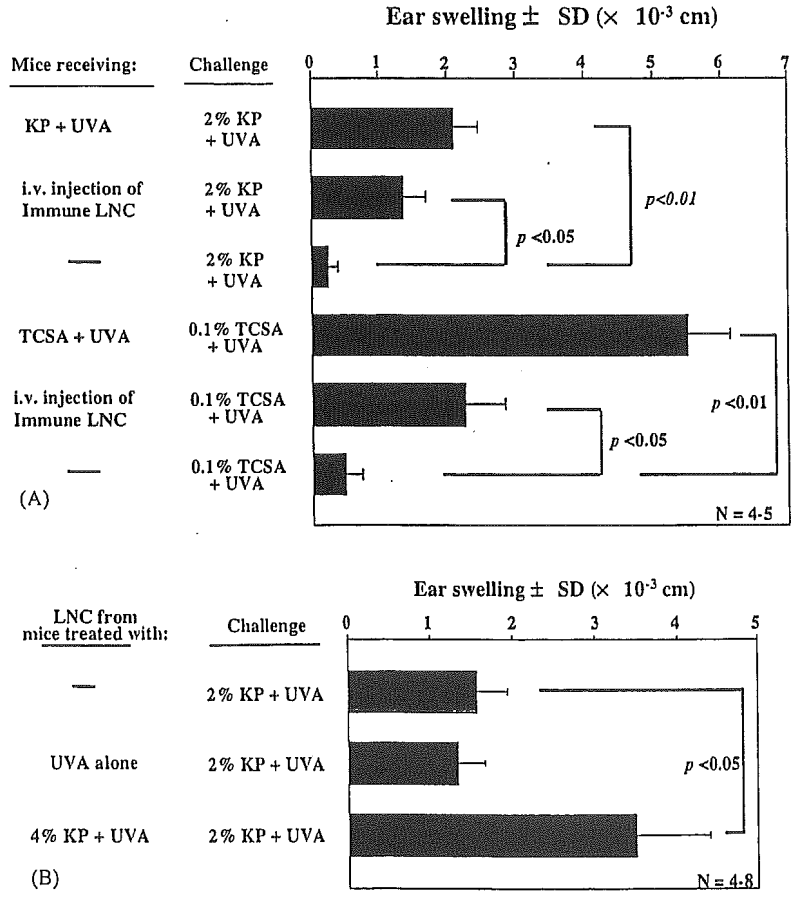

Fig. 4 (A) and (B) Transfer of LNC from KP- or TCSA-photosensitized mice. AKR/N (for KP) and BALB/c (for TCSA) mice were injected i.v. with immune LNC (2 × 10^7 cells/mouse) from KP- or TCSA-photosensitized mice. The control mice were not injected. Within 1 h after cell transfer, the recipient and control mice were challenged with 2% KP plus 20 J/cm^2 UVA or 0.1% TCSA plus 20 J/cm^2 UVA, and ear swelling response was measured after 24 h. Each column represents the mean ± S.D.